Article

In Vitro and In Vivo Studies on a Mononuclear Ruthenium Complex Reveals It is a Highly Effective, Fast-Acting, Broad-Spectrum Antimicrobial in Physiologically Relevant Conditions

Adam M. Varney, Kirsty L. Smitten, Hannah M. Southam, Simon D. Fairbanks, Craig C. Robertson, Jim A. Thomas,* and Samantha McLean*

Read Online

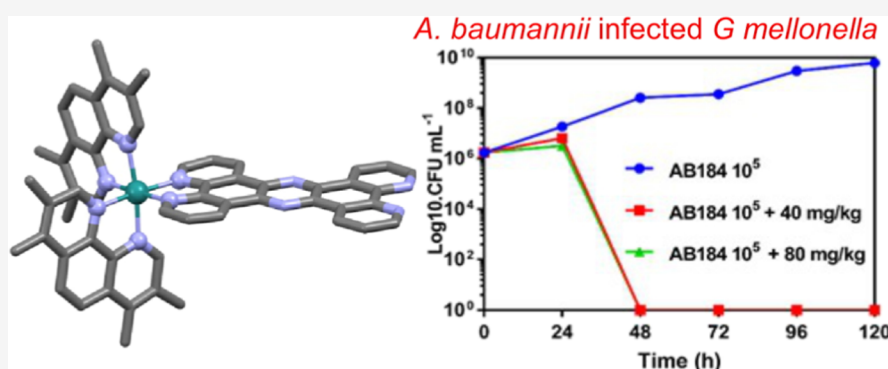ACCESS | Metrics & More | Article Recommendations | Supporting Information

A. baumannii infected G mellonella

ABSTRACT: The crystal structure of a previously reported antimicrobial Ru^{II} complex that targets bacterial DNA is presented. Studies utilizing clinical isolates of Gram-negative bacteria that cause catheter-associated urinary tract infection, (CA)UTI, in media that model urine and plasma reveal that good antimicrobial activity is maintained in all conditions tested. Experiments with a series of *Staphylococcus aureus* clinical isolates show that, unlike the majority of previously reported Ru^{II}-based antimicrobial leads, the compound retains its potent activity even in MRSA strains. Furthermore, experiments using bacteria in early exponential growth and at different pHs reveal that the compound also retains its activity across a range of conditions that are relevant to those encountered in clinical settings. Combinatorial studies involving cotreatment with conventional antibiotics or a previously reported analogous dinuclear Ru^{II} complex showed no antagonistic effects. In fact, although all combinations show distinct additive antibacterial activity, in one case, this effect approaches synergy. It was found that the *Galleria Mellonella* model organism infected with a multidrug resistant strain of the ESKAPE pathogen *Acinetobacter baumannii* could be successfully treated and totally cleared within 48 h after a single dose of the lead complex with no detectable deleterious effect to the host.

KEYWORDS: AMR, ruthenium, combinatorial therapy, ESKAPE, Galleria

1. INTRODUCTION

Although the occurrence of antimicrobial resistance was observed almost immediately after penicillin was introduced, the healthy antibiotic developmental pipeline at the time kept medicine ahead of the problem.[1−6] However, over the last 75 years, the overuse and misuse of antibiotics has created a selection pressure that has accelerated the evolution of antimicrobial resistance, AMR.[7−12] This process has been acerbated by the COVID-19 pandemic;[13,14] with up to 47% of inpatients treated for COVID-19 also contracting secondary bacterial infections,[15−18] the routine use of antibiotics as cotreatments soared.[19] A multicenter study reported that ~60% of patients admitted with COVID-19 received antibiotics at admission[20] while a study involving patients in intensive care due to SARS-CoV-2 infection showed that >90% were cotreated with antibiotics.[21]

Simultaneously, the development pipeline for new antimicrobials is running dry.[22−25] The newest class of antibiotics in current use was discovered 40 years ago[26] and the latest WHO annual pipeline report[27,28] describes only 27 new compounds being clinically investigated as potential treatments for its critical priority pathogens (compared to >5700 compounds currently in development as anticancer therapeutics[29]). More disturbingly, only six of the 27 compounds offer
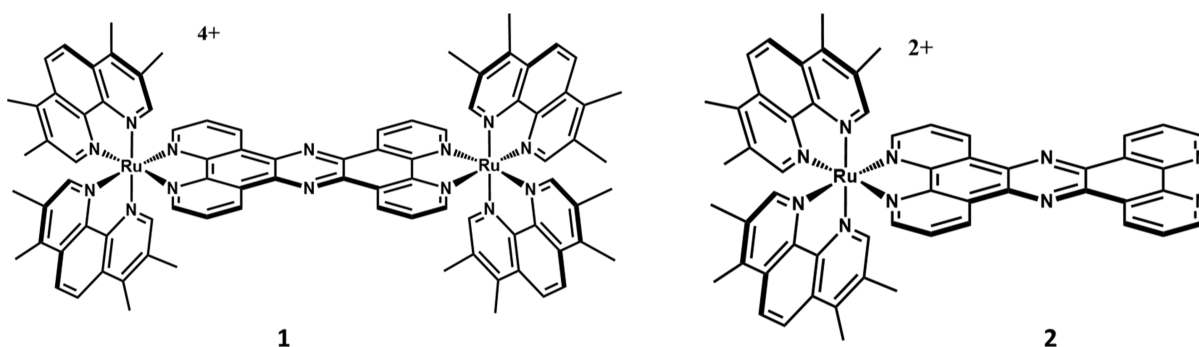
ACS Publications

A

Figure 1. Structures of therapeutic leads discussed in this report. The compounds were studied as chloride salts.
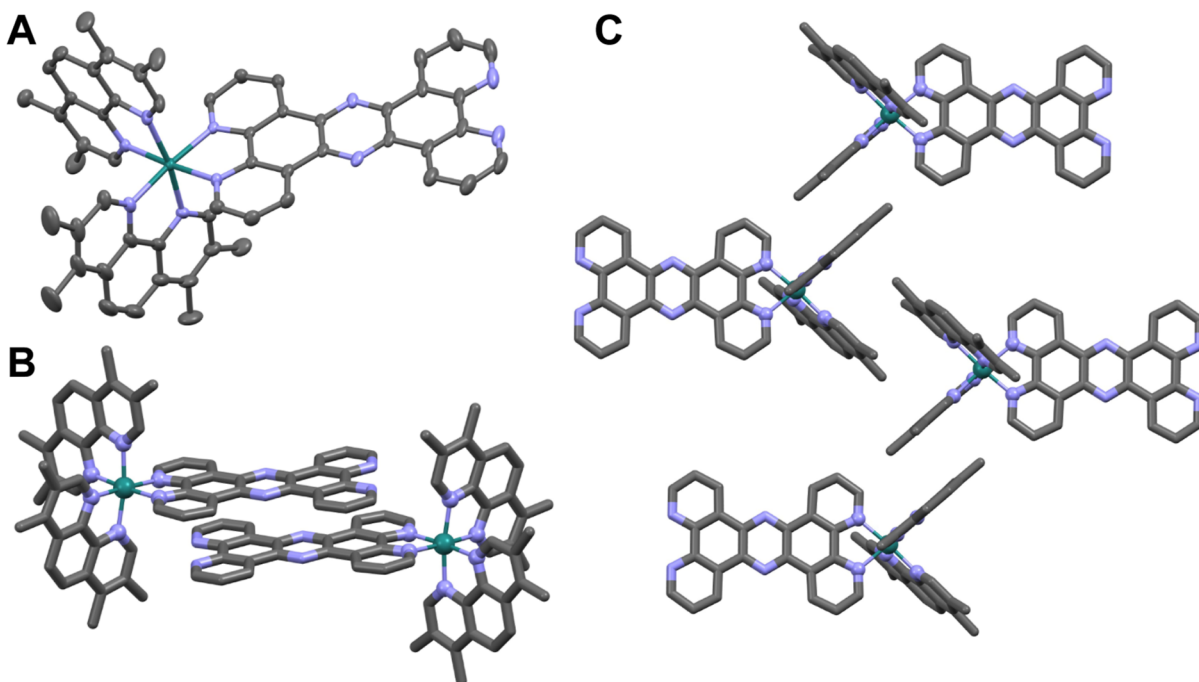

Figure 2. Selected details from the [2]Cl₂ crystal structure. (A) Thermal ellipsoid of the **2** cation. (B) Head-to-tail stacking involving tpphz ligands. (C) Tetramethyl-phenanthroline ligands participate in parallel 4-fold aryl embraces/offset face-to-face interactions. Color key: green = ruthenium, gray = carbon, blue = nitrogen.

any novelty in terms of mode of action or molecular architecture and merely two of these are being investigated as potential treatments for critical priority Gram-negative pathogens.[28−30]

These alarming circumstances have prompted new investigations into the potential antimicrobial properties of metal complexes.

Strictly speaking such research is a return of attention to this class of compounds; for example, the antimicrobial action of silver was exploited in the classical era and the medicinal use of its salts was well established by medieval times.[31,32] Indeed, the first ever synthetic antimicrobial, which proved to be a selective and highly successful treatment for syphilis, was the arsenical Salvarsan.[33,34] And, although it went on to be successfully exploited as an anticancer therapeutic,[35−37] the biological activity of cisplatin was first reported in the context of its bacteriostatic activity against *Escherichia coli*.[38] Most relevant to this report was ground-breaking work by the Dwyer group showing that polypyridyl complexes of ruthenium and other transition metals were active against a range of pathogens.[39]

These studies even led to clinical trials on this class of compounds as topical treatments for skin infections.[40,41]

More recently, the Collins and Keene groups resurrected interest in such systems by carrying out a series of investigations into the antimicrobial activity of oligonuclear Ru[II] and Ir[III] complexes related to the Dwyer prototypes, discovering that these systems were particularly active against Gram-positive bacteria.[42−44] This inspired a large number of studies on similar complexes,[45−50] but again in virtually all such cases, activity against Gram-negative species is considerably lower or entirely lacking.

As part of a program of studies on photoactive complexes as sensors and probes,[51−54] therapeutics,[55−59] and theragnostics,[60,61] the Thomas group recently derivatized a dinuclear Ru[II] complex originally developed as a nontoxic imaging probe for eukaryotic cell nuclei to yield a highly active broad-spectrum antimicrobial, **1**, Figure 1, capable of clearing ESKAPE pathogen infection in vivo.[62,63] Using the imaging capability of **1**, its mechanism of action was found to involve bacterial cell membrane disruption.[62,64] In a preliminary follow-on study, we recently showed that **2**, a mononuclear

Table 1. Minimum Inhibitory and Bactericidal Concentrations of 2 in Multiple Physiologically Relevant Media When Tested Against Clinically Isolated (CA)UTI Bacterial Pathogens[a]

strain	gDMM		PLM		AUM	
	MIC (μM)	MBC (μM)	MIC (μM)	MBC (μM)	MIC (μM)	MBC (μM)
Escherichia coli MG1655	1.56	1.56	1.30	25.00	12.50	16.67
Escherichia coli EC958	3.13	5.21	1.56	12.50	12.50	33.33
Klebsiella quasipneumoniae 18Y000138	5.21	6.25	12.50	50.00	50.00	50.00
Klebsiella pneumoniae 18Y001710	1.56	5.21	3.13	20.83	41.67	41.67
Enterobacter roggenkampii 18Y001733	3.13	5.21	6.25	37.50	6.25	33.33
Enterobacter hormaechei 19Y000094	3.13	8.33	6.25	12.50	25.00	33.33
Enterobacter hormaechei 19Y000373	2.08	5.21	5.21	12.50	6.25	25.00
Escherichia coli 20Y000092	N/A	N/A	1.56	12.50	3.13	33.33

[a]Strains were obtained from Nottingham University Hospitals Pathogen Bank, NUH identifies are provided. *N* = 3, standard deviation provided in Table S2.
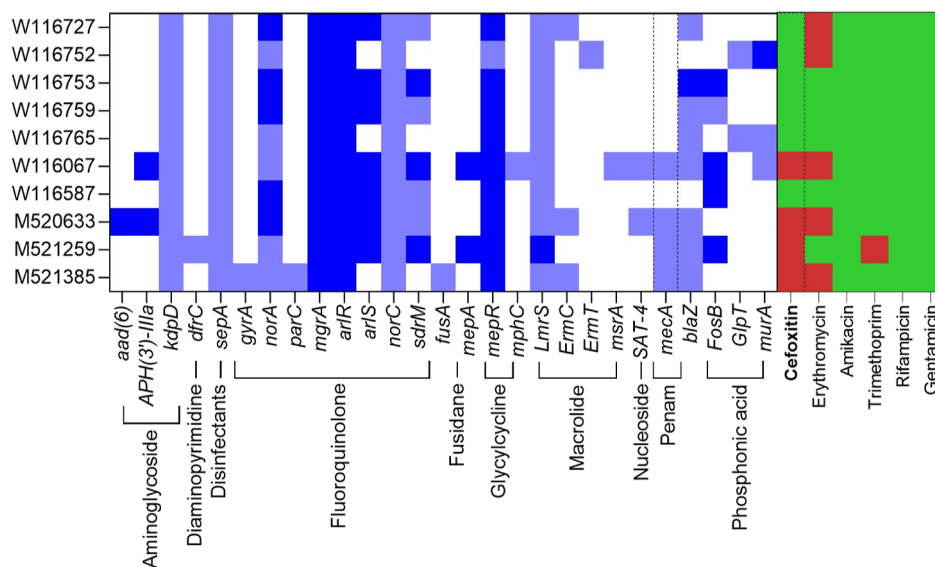

Figure 3. Antibiotic resistance profiles of ten *Staphylococcus aureus* clinical isolates. The whole genome sequences were analyzed for the presence of antimicrobial resistance genes and aligned with phenotypic antibiotic resistance testing data (EUCAST). Dark blue—CARD predicated resistance (perfect), light blue—CARD precited resistance (strict >90%), red—phenotypically resistant, green—phenotypically sensitive. Presence of *mecA* and corresponding cefoxitin resistance are highlighted in dashed boxes.

analogue of this lead, is also active but through an entirely different mechanism of action.[65] Unlike 1, the mononuclear complex does not disrupt cell—wall structure but is cell permeant and once internalized binds to bacterial DNA. This proposed mechanism of action is distinct from DNA targeting antibiotics such as (fluoro)quinolones that target topoisomerase activity[66] and the sulphonamides and diaminopyrimidines that target tetrahydrofolate production.[67] As direct DNA-targeting is a neglected mechanism of action, particularly for a broad-spectrum antimicrobial,[68,69] herein we report on investigations into the application of 2 as a therapeutic for a range of pathogenic Gram-positive and Gram-negative bacteria in different media and pH conditions, as well as in an in vivo model. Using a selected group of conventional antibiotics and complex 1, we also assess its potential to be used in a combinatorial therapeutic regime.

2. RESULTS AND DISCUSSION

2.1. Crystal Structure of Complex 2.
X-ray quality crystals were grown by vapor diffusion of diethyl ether into a methanol solution of [2]Cl₂ (Figure 2). The packing of cations within this structure is due to noncovalent motifs involving

coordinated aromatic ligands. Pairs of 2 stack through a head-to-tail offset arrangement involving their extended tpphz ligands (Figure 2b), while the tetramethyl-phenanthroline ligands of adjacent cations participate in characteristic parallel 4-fold aryl embraces/offset face-to-face interactions (Figure 2c).

Having confirmed the structure of 2, its chloride salt was then used for a detailed investigation into its antimicrobial activity.

2.2. Antimicrobial Activity in Different Media.
Previous studies on metal complex therapeutic leads, including 1, have shown that apparent activity is often dependent on the medium composition, which may have implications for clinical efficacy. Consequently, we investigated whether this effect was observed for 2. As it was already established that the complex is active against pathogenic *E. coli* and *Staphylococcus aureus* species,[65] its efficacy against a panel of previously characterized (Catheter Associated) Urinary Tract Infection ((CA)UTI) clinical isolates in different media was explored.[70] Three different media were used; glucose-defined minimal medium (gDMM),[62] and two physiologically relevant media; artificial urine medium (AUM)[71] and plasma-like medium (PLM).[72,73]

Table 2. Activity of Complex 2 Against a Range of Clinically Isolated AMR Strains of *S. aureus* Including MRSA

strain/ID[a]	origin	chemically defined medium		plasma-like medium	
		MIC (μM)	MBC (μM)	MIC (μM)	MBC (μM)
S. aureus	ATCC 29213	1.56	2.34	0.20	2.60
S. aureus USA300	LAC JE2[b]	1.56	1.56	0.20	6.25
S. aureus W116727	wound	1.56	1.56	0.20	3.13
S. aureus W116752	wound	1.43	0.91	0.24	12.50
S. aureus W116753	wound	0.91	1.56	0.37	6.25
S. aureus W116759	wound	1.56	1.56	0.24	4.43
S. aureus W116765	wound	1.56	6.25	0.33	5.21
MRSA W116067	wound	1.56	1.56	0.20	6.51
S. aureus W116587	wound	1.56	1.56	0.33	6.77
MRSA M520633	patient swab	1.30	1.56	0.39	3.39
MRSA M521259	patient swab	1.56	1.56	0.20	4.17
MRSA M521385	patient swab	0.78	0.91	0.20	4.17

[a]Strains were obtained from Chesterfield Royal Hospital, hospital identifiers are provided. $N = 3$ SD is presented in Table S4 represented in Supporting Information. MRSA classification was determined via presence of *mecA* gene. [b]See ref 79.
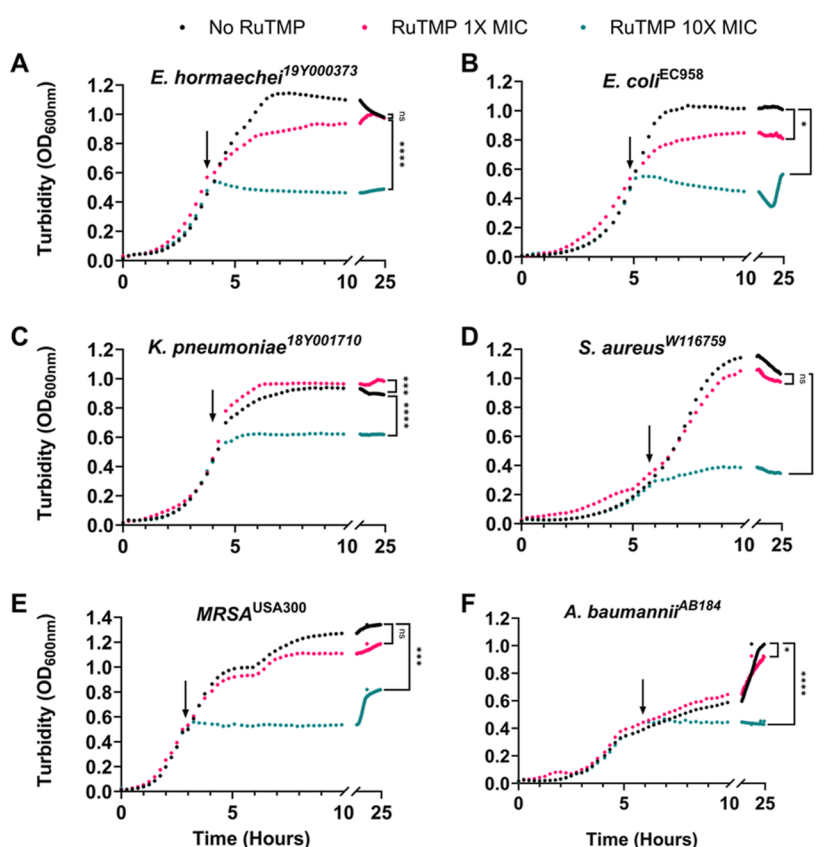

Figure 4. Complex **2** shows growth inhibition of multiple pathogens at early exponential growth phase. Cultures were grown to early exponential phase 37 °C and 475 CPM shaking in 24-well plates in gDMM (A−C), CDM (D,E), gDMM + 1× MEM (F). Upon reaching early exponential phase (OD$_{600\ nm}$ 0.4−0.5), 1× or 10× the MIC of the complex or vehicle control was injected and growth monitored at 15 min intervals across the 24 h time course. $N = \geq 6$. One-way ANOVA was performed on final culture turbidity's with Dunnett's multiple comparisons test. Significance levels: not significant (ns, $p \geq 0.05$), * ($p < 0.05$), ** ($p < 0.01$), *** ($p < 0.001$), and **** ($p < 0.0001$).

The two clinically relevant media mimic the environment that (CA)UTI strains are likely to encounter during infection and are also standardized to prevent batch-to-batch variation. Selected results from these experiments, which involved a range of (CA)UTI isolates, are summarized in Table 1 (see Table S1 for the full set of bacterial strains tested).

Comparing the minimal inhibitory concentration (MIC) of **2** in gDMM and PLM showed minimal variation, with MICs remaining low across the different (CA)UTI strains. When

tested in AUM, the strains demonstrated less sensitivity to the compound; with *Klebsiella pneumoniae* (18Y000138) having the highest MIC of 50 μM ($\sim$51 mg L^{-1}), however, this is still a clinically appropriate concentration of antimicrobial for therapy. That these strains remain sensitive to **2** in multiple clinically relevant media suggests that their efficacy will be unimpaired during the treatment of an infection under physiological conditions. Despite the range of multidrug resistance mechanisms and virulence factors within this panel
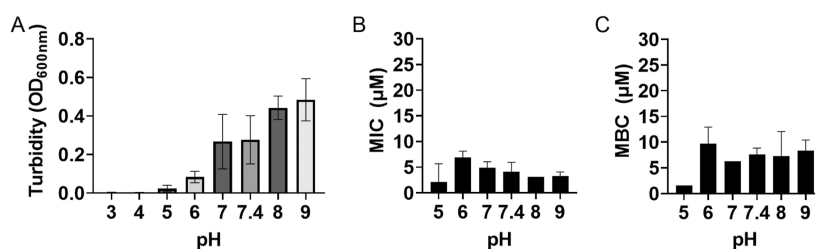
Figure 5. Complex **2** remains inhibitory and bactericidal against *E. coli* EC958 across a broad pH range (5−9). (A) Turbidity readings ($OD_{600 nm}$) were taken from a 96-well plate after static incubation in gDMM at 37 °C for 18 h. (B) Minimal inhibitory concentration testing was performed at under the same conditions as (A) through a pH range of 5−9. (C) Minimal bactericidal concentration assays were performed by spotting 10 μL of all MIC wells with no growth onto Mueller−Hinton agar and incubation at 37 °C for 24 h prior to identification of growth. $N \geq 3 \pm$ SD. No statistically significant difference was observed between pH's 6−9 for either the inhibitory nor bactericidal assays (one-way ANOVA: $P > 0.05$).

of clinical isolates,[70] no strain displayed significantly increased resistance to the complex, suggesting that none of their existing resistance mechanisms cause cross-resistance to **2**. Significantly, this sensitivity was observed across an extended panel of clinical isolates from multiple infection types and genera including *Pseudomonas* sp., *Salmonella* sp., *Citrobacter* sp., *Acinetobacter* sp., and *Serratia* sp., all of which had MICs below 8 μM (8.21 mg/L, Table S1).

2.3. Activity Against *S. aureus* Clinical Isolates.
Resistant strains of *S. aureus* are prominent Gram-positive members of the WHO priority pathogen list. They cause a range of infections, including skin and soft tissue infections, and despite screening and isolation of patients, nosocomial MRSA still poses a serious threat to global healthcare systems. However, apart from some notable exceptions,[68,74−76] previous studies on ruthenium-based antimicrobials have frequently revealed increased resistances of MRSA strains compared with methicillin sensitive strains.[42,77,78] Consequently, having confirmed that **2** displays a breadth of activity across Gram-negative pathogens in physiologically relevant conditions, we then investigated its potency across a range of clinical isolates of *S aureus*. To assess the effectiveness of **2** against both methicillin sensitive and methicillin resistant strains of *S aureus*, a panel of ten clinically isolated strains were obtained and assessed phenotypically and genotypically for antimicrobial resistance. Of the ten isolates, four were classified as methicillin resistant and six as methicillin sensitive based on the presence of the *mecA* gene, which was subsequently confirmed by a cefoxitin disk diffusion assay (Figure 3). In fact, the strains display resistance to a spectrum of different antibiotics, and the Comprehensive Antibiotic Resistance Database Resistance Gene Identifier suggests that a range of antimicrobial resistance genes are involved (Figure 3).

As the sensitivity of *S. aureus* to **2** in defined minimal medium has previously been demonstrated,[65] herein the sensitivity of the ten clinical isolates, including MRSA strains, in both chemically defined medium and a physiologically relevant plasma-like medium was investigated (Table 2).

In contrast to **1**, it was found that Gram-positive *S. aureus* shows a greater sensitivity to **2** than the Gram-negative (CA)UTI pathogens tested in the same conditions. All clinically isolated *S. aureus* strains showed similar levels of sensitivity to **2**, despite their differing AMR and virulence profiles (Figures 3 and S1 and Table S3), and crucially the sensitivity of *S. aureus* isolates to **2** was the same in both MRSA and methicillin sensitive strains offering evidence that its efficacy would be unaltered in a clinical setting against a wide

variety of pathogens and highlighting its potential in the treatment of MRSA infections.

2.4. Complex 2 is Active Against Pathogens in Early Exponential Growth Phase. Although the inhibitory and bactericidal effectiveness of **2** was estimated using standard MIC methodology, this requires low initial turbidity cultures and dilution from a stationary phase; yet, in a clinical setting, antibiotic treatment is often administered when the bacterial load is high and/or the infective isolate is actively growing. To better understand the effectiveness of **2** against actively growing bacterial cultures in a more clinically relevant setting, we exposed clinical isolates in early exponential growth phase to complex **2** at 1× and 10× their minimal inhibitory concentrations.

In these conditions, unlike previous studies on **1**,[63] there was no delayed inhibition of growth upon exposure to **2** (Figure 4). Here, exposure to ten times the minimal inhibitory concentration of **2** caused a significant decrease in final carrying capacity of all tested species ($p < 0.001$). This demonstrates the rapid activity of **2** in preventing growth of both Gram-positive and Gram-negative bacterial pathogens.

2.5. Bacterial Sensitivity to Complex 2 Across a pH Range. Physiological conditions encountered during infection provide a range of pH environments, including: skin pH (∼4−6), infected wounds (∼7), urine (∼4.5−8), UTI urine (∼8.5−9), and the rapidly changing environment of the gastrointestinal tract: from the highly acidic stomach (∼1.5−3) with variable pH through the duodenum (∼6), small intestine (∼6−7.4), cecum (∼5.7), and rectum (∼6.7). Organisms such as *E. coli* are likely to encounter these conditions during infection, particularly *E. coli* in the urinary and gastrointestinal tracts. Consequently, if complex **2** is to be delivered systemically, it will likely encounter a range of pH's. Therefore, the inhibitory and bactericidal activity of **2** against a clinically isolated *E. coli* was investigated over a wide pH range. *E. coli* EC958 was chosen for experimentation as it displays a general pH tolerance, and significant genotypic and phenotypic data are available for this strain, making it an appropriate model organism.

The range of *E. coli* EC958 acid tolerance was confirmed by overnight growth. The strain grew between pH's 5−9, with decreasing turbidity observed in increasingly acidic conditions and no growth detected at pH 4 or below (Figure 5a). We therefore tested inhibitory and bactericidal concentrations between pH's 5−9. The minimum inhibitory and bactericidal concentrations of **2** against *E. coli* EC958 remained stable at all pHs tested suggesting that the complex will retain activity in diverse physiological conditions (Figure 5b,c).

2.6. Combinatorial Effects with Conventional Antibiotics.

Dual antibiotic treatments are frequently used to treat severe infections, such as bacteremia and sepsis, particularly when caused by Gram-negative pathogens, including the ESKAPE pathogens. Effective combination therapies should use antimicrobials that are not antagonistic but display additive activity or synergy to assist in the clearance of infections. If antagonistic combinations are used, not only will such treatments likely fail but they could also facilitate the emergence of further antibiotic resistance. We therefore assessed the therapeutic action of **2** in vitro as a component of combination therapies with commonly used antibiotics. Five antibiotics were selected for testing against *E. coli* EC958 using EUCAST standard guidelines to determine the precise clinical sensitivity of the strain in Mueller−Hinton broth and gDMM, which was used as a reference for the synergy assay. *E. coli* EC958 was clinically resistant to β-lactam and quinolone antibiotics and exhibited high levels of resistance to cephalexin, ampicillin, and ciprofloxacin (Table S6). When tested in gDMM some decreased resistance to these three antibiotics was observed. *E. coli* EC958 was categorized as sensitive to Meropenem and nitrofurantoin in accordance with EUCAST guidelines.

Following MIC testing, **2** was assessed for antagonism or synergy in combination with the conventional antibiotics and dinuclear complex **1** by assessing their fractional inhibitory concentration, FIC. Checkerboard assays, performed in gDMM, showed that all tested combinations of antibiotics with **2**, including its dinuclear analogue, were additive (FIC index 0.5−4), with no evidence of antagonism in any of the combinations (Table 3). Notably, the combination of

Table 3. Assessing the Therapeutic Interaction of Complex 2 with the Antibiotics Used in Combination Therapies

antibiotic	FIC index	antagonistic/additive/synergistic
Meropenem	0.58 ± 0.22	additive
Ampicillin	1.01 ± 0.00	additive
CEF	1.00 ± 0.00	additive
Ciprofloxacin	0.68 ± 0.19	additive
Nitrofurantoin	1.08 ± 0.19	additive
1	0.91 ± 0.16	additive

Meropenem and **2** had the lowest FIC index (0.58) exhibiting pronounced additive effects close to synergy ($\leq$0.5). The observation of an additive effect on cotreatment with **1** and **2** confirms that the two complexes display different mechanisms of action. Overall, these encouraging observations indicate that **2** offers great potential for use in combination therapy and would not interfere with the administration of extant antibiotics.

2.7. In Vivo Efficacy Studies of Complex 2 Against the ESKAPE Pathogen *Acinetobacter baumannii*.

Although the in vitro studies presented above demonstrate that **2** clearly displays potential as a broad-spectrum antimicrobial active in a range of physiologically relevant conditions, these results may not be fully indicative of the activity of the compound in vivo. This is why, prior to their move into human studies, the efficacies of leads are usually studied in mammalian or insect models. Commonly, infection models are studied within rodent or zebrafish models prior to moving to large mammalian models. However, recently there has been an

increase in the use of *Galleria mellonella* (greater wax moth larvae) in toxicology screening and as an infection model.[80−83]

Apart from lower costs and greater convenience of *G. mellonella* compared to traditional mammalian models, it presents ethical and logistical advantages in the context of the move toward the reduction, refinement, and replacement, 3Rs, of animal testing. One further attraction of *G. mellonella* is that, unlike other nonvertebrate models, but similar to mammals, it has an innate immune system comprising humoral and cellular responses.[80,84−86] This means there is a good correlation between bacterial virulence in mammals and the *Galleria* model, which has been successfully exploited to study the pathogenesis and treatment of bacterial infections and give information about potential dosing for future preclinical and clinical studies. In a recent report, we described the use of *G. mellonella* as an infection model to study the antimicrobial efficacy of **1** against multidrug resistant *A. baumannii* infections[87] and as a previous toxicology screen[65] had shown that **2** is nontoxic to *Galleria* up to concentrations of at least 80 mg kg^{-1}—we set out to investigate the potential of the complex to act as an in vivo treatment for *A. baumannii* and to compare the reported activity of **2** to that of **1** in the same in vivo infection model.

A. baumannii is a member of the ESKAPE group of bacterial pathogens causing hospital acquired infections and carbapenem resistant strains were classified by the WHO as "Priority 1: critical" in urgent need of research and development of new antimicrobials.[88,89] An extensive range of antibiotic resistance genes are present within the *A. baumannii* pan genome, and multidrug resistant strains are widespread across the globe. In addition, extensively drug-resistant and pan drug resistant strain prevalence is also increasing at an alarming rate. Indeed, in many regions of the world, carbapenem resistant *A. baumannii*, CRAB, strains are now the most commonly encountered form of this pathogen.[90] Clinical manifestations of CRAB range from urinary and respiratory tract infections to bacteremia and meningitis and such infections often lead to high mortality rates (>30%).[91,92] Furthermore, thanks in part to COVID-associated superinfection, nosocomial CRAB is increasingly becoming associated with ventilator acquired pneumonia.[90]

The *G. mellonella* model we have developed uses a multidrug resistant CRAB, the AB184 strain, which is representative of one of the most common *A. baumannii* clonal groups in both the UK and the USA.[87,93] In the current studies, larvae were injected with AB184 at two different concentrations (10^5 or 10^6 CFU mL^{-1}). After 30 min, infected larvae were then treated with a single dose of either 40 or 80 mg kg^{-1} of **2** and results were compared to untreated controls. As in previous studies, apart from mortality, the effects of exposure to **2** on the health of larvae was monitored through activity and melanization scoring over the course of the experiment. To ensure that the observed difference between survival of the coinjected larvae and the bacteria injected controls was a direct result of infection clearance, the bacterial load in the larval hemolymph was monitored over the 120 h experiment (Figure 6a).

Survival curves associated with these experiments (Figure S2) were plotted for treated infected larvae and compared to water and AB184 only controls; controls using uninfected larvae that were treated with **2** were also carried out, and as observed in a previously reported toxicity screen, these revealed no detectable toxic effects at either concentration.
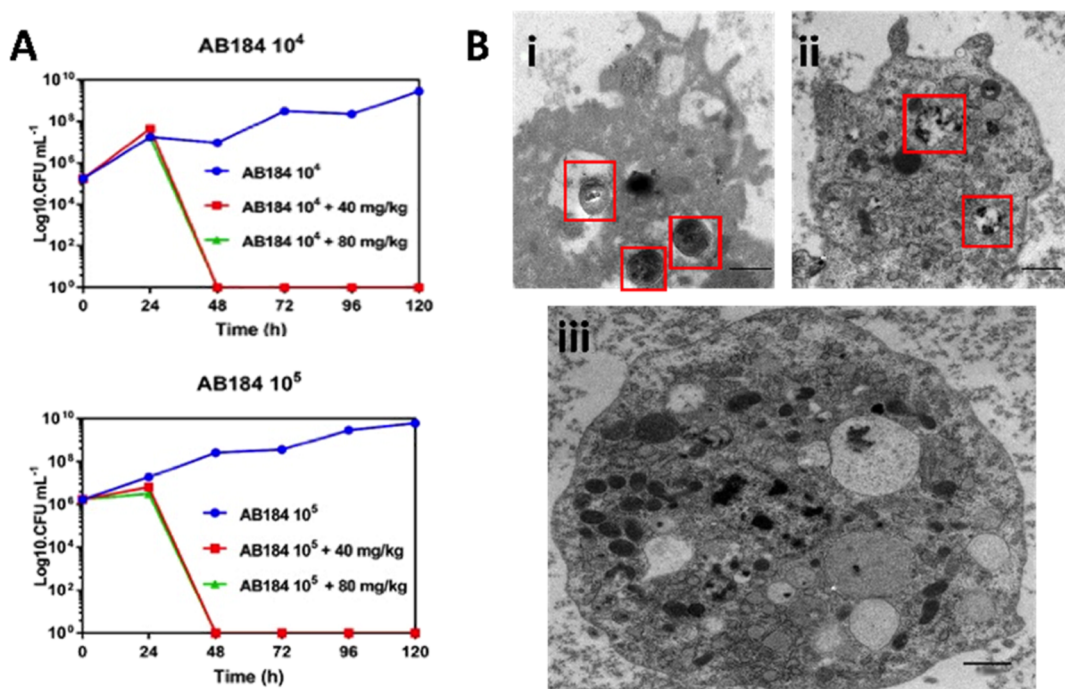
Figure 6. (a) *G. mellonella*-based infection model. Larvae were first exposed to *A. baumannii* at 10^4 CFU mL^{-1} (top) or 10^5 CFU mL^{-1} (bottom), then injected with 40 mg kg^{-1} or 80 mg kg^{-1} of **2**. (b) TEM of hemolymph extracted from *G. mellonella* at 24 and 48 h post inoculation with *A. baumannii* and **2**. Protocol: Larvae were injected with bacteria in their right pro-leg. Treated *Galleria* received a dose of the complex 30 min later in their left pro-leg. Larvae were incubated for 120 h at 37.5 °C.

In contrast to the untreated control group of larvae, where continual exponential increase in AB184 bacterial colonies was observed over 120 h, either dose regimen of **2** resulted in the total eradication of AB184 infection in all treated larvae between 24 and 48 h (Figure 6a).

Strikingly, this rate of clearance is considerably faster than that observed for **1**, which in identical conditions took 96 h to clear the same *A. baumannii* infection. Furthermore, whereas previous statistical analyses have confirmed that AB184 is pathogenic to *G. mellonella* at concentrations 10^5 CFU mL^{-1} and above, log-rank *t* tests performed on the survival curves for AB184 infected larvae (40 and 80 mg kg^{-1}) treated with **2** showed no significant difference between the treated larvae and the water controls (concentrations 10^5, 10^6: 40 mg kg^{-1} *P* = 0.0554 and 0.0549 and 80 mg kg^{-1} *P* = 0.1385 and 0.1380). This analysis indicates that the complex is an effective treatment for larval CRAB infection in this model organism. Further evidence confirming the clearance of the infection was provided by the intrinsic imaging properties of the complex.

As complex **2** contains an electron dense ruthenium center, it is an effective contrast stain for transmission electron microscopy, TEM, and using this property, hemolymph from infected larvae treated with **2** was extracted at 24 and 48 h post treatment (Figure 6b). The resultant images confirmed that **2** is preferentially taken up by *A. baumannii* cells, as they displayed more pronounced contrast than host cells. Although *A. baumannii* cells were detectable within the extracted hemolymph and in hemolymphocyte cells to 24 h, the hemolymphocyte cells had phagocytosed the bacteria in a manner that is analogous to macrophages and neutrophils. At 48 h, not even dead bacterial cells were observed within hemolymph and hemocyte cells and the hemocyte cells had a healthy morphology. In comparison, although complex **1** also effectively treated infection at similar concentrations total

clearance of *A. baumannii* from larvae was only observed after 96 h of exposure.[87]

3. CONCLUSIONS

Although the increasingly urgent global health challenge of treating AMR pathogens is revitalizing fundamental research into the development of antimicrobials, entirely new molecular scaffolds toward these goals are still severely lacking. This is reflected in the fact that despite the increased activity in this arena, there is still a dearth of genuinely innovative broad-spectrum antimicrobials entering the development pipeline. In this study, we carried out a detailed assessment into a recently identified potential therapeutic lead for AMR pathogens. These studies show that the complex is highly active against a range of multidrug-resistant strains of Gram-negative (CA)UTI and ESKAPE pathogens, including clinical isolates from multiple infection types and genera. Complex **2** is a genuine broad-spectrum antimicrobial displaying comparable activity against clinical isolates of resistant *S. aureus* strains in physiologically relevant media. Unlike many previously reported Ru^{II}-based complexes, **2** even retains its potent activity against MRSA strains, and in media and pHs that represent a range of physiologically relevant environments, it continues to display efficacy against both Gram positive and Gram negative bacteria. Encouragingly, cotreating bacteria with complex **2** and established antibiotics or its dinuclear analogue, **2** produced no antagonistic effects but consistently resulted in markedly additive effects, which in the case of Meropenem borders into synergy. Furthermore, a single dose of the complex directly images and completely clears an AMR strain of *A. baumannii* from *G. mellonella*, an infection the intrinsic immune system of the model organism is incapable of clearing by itself. This successful treatment has no detectable deleterious effect on *Galleria* larvae and requires concen-

trations that are considerably lower than those tolerated by this model. Interestingly, total clearance of the bacteria occurs in <48 h, which is considerably faster (∼96 h) than equivalent treatment with **1**. This effect and the observation that it continues to be active during bacterial early exponential growth phase, means that **1** may be suited to shorter treatment courses, a type of regime that has been identified as optimizing cure rates and minimizing the potential for bacterial resistance acquisition.[94,95]

Taken together, the findings in this study provide clear evidence that complex **2** offers considerable potential as a novel broad-spectrum antimicrobial. Although a previous report has established that this complex targets bacterial nucleic acids,[65] extensive experiments to delineate the exact details of its mechanism of action at a molecular level are currently underway and these will form the basis of a forthcoming study.

4. EXPERIMENTAL SECTION

4.1. Bacterial Strains and Growth. Growth was achieved in Mueller–Hinton broth, glucose containing defined minimal medium,[62] chemically defined medium[64] plasma-like medium,[72,73] or artificial urine medium[71] made up as per manufacturer's instructions or as described in the literature using standard techniques. Strains were obtained from The McLean culture collection, Chesterfield Royal Hospital, UK and Nottingham University Hospitals Trust Pathogen Bank, UK.

4.2. Preparation and Storage of Complex 2. The complex was synthesized as previously described.[65] Stock solutions were made to a concentration of 5 mg mL^{-1} in sterile deionized water and stored at room temperature and protected from light.

4.3. Crystal Structure of 2. X-ray quality crystals of [**2**]Cl$_2$ were grown by slow evaporation of an ethanol/acetone solution. Details of its empirical formula and structural refinement are in Table 4. More details of bond angles and lengths are available in the CIF file (CCDC 2354069) deposited with the Cambridge Crystallographic Data Centre.

4.4. Bioinformatic Analysis of *S. aureus* Strains. Genomic DNA was extracted from cell pellets using a genomic DNA isolation kit (Merck) as per manufacturer's instructions. DNA quality was checked using a NanoDrop microvolume spectrophotometer (ThermoFisher Scientific) and quantified using a Qubit 4 fluorometer (Invitrogen) high sensitivity dsDNA assay kit. Strains were sequenced on the Illumina HiSeq/NovaSeq platform and assembled by a MicrobesNG (Birmingham, UK). General features of the isolates are summarized in Table S5. The genomic data generated during this study are available in the National Center for Biotechnology Information BioProject: PRJNA1069650. BioSample accession numbers: SAMN39618626-36. SRR raw Illumina data: SRR28824215-25. Annotated genomes are available in figshare. Antimicrobial resistance markers were identified using Resistance Gene Identifier (RGI) v6.0.0 tool of the Comprehensive Antibiotic Resistance Database (CARD) v3.2.5.[96] Only resistance genes that showed a perfect or strict match with coverage for a given gene and achieved ≥90% identity and read length in the database were included in this study. The Virulence Factor Database platform VFAnalyzer was used to predict virulence factors present within the draft genomes.[97] Phage elements were predicted using PHAST-EST[98]

Table 4. Crystal Data and Structure Refinement

identification code	iaj713k_0m
empirical formula	C$_{59}$H$_{56}$Cl$_2$N$_{10}$O$_3$Ru
formula weight	1125.10
temp, K	100
crystal system	triclinic
space group	$P\bar{1}$
a, Å	13.6538(16)
b, Å	14.1267(17)
c, Å	15.5268(18)
α, deg	98.318(3)
β, deg	93.030(3)
γ, deg	92.277(4)
vol, Å^3	2955.8(6)
Z	2
ρ_{calc}, g/cm^3	1.264
μ, mm^{-1}	0.406
F(000)	1164.0
crystal size, mm^3	0.4 × 0.35 × 0.15
radiation	Mo Kα (λ = 0.71073)
2θ range for data collection, deg	5.346 to 56.926
index ranges	$-18 \leq h \leq 18, -18 \leq k \leq 18, -20 \leq l \leq 20$
reflections collected	64,507
independent reflections	14,811 [R_{int} = 0.0472, R_{sigma} = 0.0449]
data/restraints/params	14,811/661/700
goodness-of-fit on F^2	1.058
final R indexes [$I \geq 2\sigma(I)$]	R_1 = 0.0567, wR_2 = 0.1557
final R indexes [all data]	R_1 = 0.0763, wR_2 = 0.1717
largest diff. peak/hole, e Å^{-3}	1.17/−0.88

4.5. Minimal Inhibitory and Bactericidal Assays. MIC assays were performed as previously described. Following the MIC assay, 10 μL from each well displaying no visible growth was transferred to an MHA plate, along with a positive growth control. Plates were incubated for 18 h at 37 °C. The lowest concentration showing no growth was recorded as the MBC.

4.6. Growth Inhibition Assays. 1 mL of growth medium was added to wells in triplicate per condition. A 1% overnight culture grown in the same medium was added to each well, excluding sterility control wells. A polyurethane Breath-Easy membrane (Merck) was applied and plates were incubated shaking using a double orbital at and 37 °C in a Cytation 3 plate reader set to take OD$_{600}$ reads every 15 min for 24 h. For assays with compound addition, when cultures reached early exponential phase (OD$_{600}$ ∼ 0.4) plates are removed varying concentrations of compound were added, a new Breath-Easy membrane was applied and plates were reincubated with measuring OD$_{600}$ every 15 min for a further 24 h.

4.7. Checkerboard Synergy Assays. Checkerboard microdilution assays were set up as previously described. FIC index (FICi) values were determined for each drug combination, with synergy recorded where the FICi < 0.5, additive recorded where the FICi value was 0.5−4, and antagonism recorded for combinations with a FICi value of >4.[99]

4.8. *G. mellonella* Assays. TruLarv *G. mellonella* were used for this study to ensure they were reared without antibiotics and were all a similar weight. For each compound concentration, seven larvae were used, and for the control, 15 larvae were used. Insects were injected on the initial day with 10 μL of the correct concentration stock solution of **2** or water (control) into their left pro-leg. Once injected larvae were

stored in a Petri dish containing filter paper and incubated at 37.5 °C. Three analysis tests were conducted at 0, 24, 48, 72, 96, and 120 h. Activity scores were recorded: 0-no movement, 1-corrects itself, 2-movement on stimulation, and 3-movement without stimulation. Live/dead scores were recorded to produce percentage survival curves. Melanization was scored on a scale of 0−4: 0—completely black, 1—black spots, 2—tail/line black and 4—none. Cocoon formation was not observed in this case. At the end of the toxicity screen *Galleria* larvae were disposed of in a humane manner.[100]

4.9. Transmission Electron Microscopy. Cells were fixed using 3% glutaraldehyde. Cells were dehydrated using a series of ethanol washes (70−100% ethanol) and TEM samples sectioned in Araldite resin by microtome. Samples were examined on an FEI Tecnai instrument operating at 80 kV equipped with a Gatan 1 K CCD camera. Images were processed and analyzed using FIJI ImageJ software.

■ ASSOCIATED CONTENT

Ⓢ Supporting Information

The Supporting Information is available free of charge at https://pubs.acs.org/doi/10.1021/acsinfecdis.4c00447.

> Further MIC data for clinical isolates of Gram negative pathogens and more CAU(TI) isolates, prophage predictions for *S. aureus* clinical isolates determined using PHASTEST, MIC, and MBC values for clinical isolates of resistant *S. aureus* clinical isolates, summary information for genomes generated from the *S. aureus* isolates and associated predicted virulence factors according to the Virulence Factor Database, summary of sensitivity of *E. coli* EC958 to clinically employed antibiotics, and Kaplan−Meier percentage survival curves for the AB184 infection model in untreated and treated *Galleria* (PDF)
>
> HPLC traces of complex **2** (PDF)

■ AUTHOR INFORMATION

Corresponding Authors

Jim A. Thomas − *Department of Chemistry, University of Sheffield, Sheffield S3 7HF, U.K.;* ⓞ orcid.org/0000-0002-8662-7917; Email: james.thomas@Sheffield.ac.uk

Samantha McLean − *School of Science and Technology, Nottingham Trent University, Nottingham NG11 8NS, U.K.;* Email: samantha.mclean@ntu.ac.uk

Authors

Adam M. Varney − *School of Science and Technology, Nottingham Trent University, Nottingham NG11 8NS, U.K.; Medical Technologies Innovation Facility (MTIF), Nottingham NG11 8NS, U.K.;* ⓞ orcid.org/0000-0002-5943-161X

Kirsty L. Smitten − *Department of Chemistry, University of Sheffield, Sheffield S3 7HF, U.K.; School of Bioscience, The University of Sheffield, Sheffield S10 2TN, U.K.*

Hannah M. Southam − *School of Bioscience, The University of Sheffield, Sheffield S10 2TN, U.K.*

Simon D. Fairbanks − *Department of Chemistry, University of Sheffield, Sheffield S3 7HF, U.K.*

Craig C. Robertson − *Department of Chemistry, University of Sheffield, Sheffield S3 7HF, U.K.*

Complete contact information is available at:
https://pubs.acs.org/10.1021/acsinfecdis.4c00447

Notes

The authors declare no competing financial interest.

■ ACKNOWLEDGMENTS

■ ABBREVIATIONS

AMR, antimicrobial resistance; AUM, artificial urine medium; (CA)UTI, (Catheter Associated); CRAB, carbapenem resistant *A. baumannii*; EUCAST, European Committee on Antimicrobial Susceptibility Testing; gDMM, glucose-defined minimal medium; MRSA, Methicillin-resistant *Staphylococcus aureus*; UTI, urinary Tract Infection; PLM, plasma-like medium.

■ REFERENCES

(1) Walsh, C. Molecular Mechanisms That Confer Antibacterial Drug Resistance. *Nature* **2000**, *406* (6797), 775−781.

(2) Alanis, A. J. Resistance to Antibiotics: Are We in the Post-Antibiotic Era? *Arch. Med. Res.* **2005**, *36* (6), 697−705.

(3) Shlaes, D. M.; Bradford, P. A. Antibiotics—from There to Where?: How the Antibiotic Miracle Is Threatened by Resistance and a Broken Market and What We Can Do about It. *Pathog. Immun.* **2018**, *3* (1), 19−43.

(4) Aminov, R. History of Antimicrobial Drug Discovery: Major Classes and Health Impact. *Biochem. Pharmacol.* **2017**, *133*, 4−19.

(5) Lewis, K. Platforms for Antibiotic Discovery. *Nat. Rev. Drug Discovery* **2013**, *12* (5), 371−387.

(6) Lewis, K. The Science of Antibiotic Discovery. *Cell* **2020**, *181* (1), 29−45.

(7) Sugden, R.; Kelly, R.; Davies, S. Combatting Antimicrobial Resistance Globally. *Nat. Microbiol.* **2016**, *1* (10), 16187.

(8) Medina, E.; Pieper, D. H. Tackling Threats and Future Problems of Multidrug-Resistant Bacteria. In *Current Topics in Microbiology and Immunology*; Springer: Cham, 2016; Vol. *398*, pp 3−33.

(9) Holmes, A. H.; Moore, L. S. P.; Sundsfjord, A.; Steinbakk, M.; Regmi, S.; Karkey, A.; Guerin, P. J.; Piddock, L. J. V. Understanding the Mechanisms and Drivers of Antimicrobial Resistance. *Lancet* **2016**, *387* (10014), 176−187.

(10) Murray, C. J.; Ikuta, K. S.; Sharara, F.; Swetschinski, L.; Robles Aguilar, G.; Gray, A.; Han, C.; Bisignano, C.; Rao, P.; Wool, E.; Johnson, S. C.; Browne, A. J.; Chipeta, M. G.; Fell, F.; Hackett, S.; Haines-Woodhouse, G.; Kashef Hamadani, B. H.; Kumaran, E. A. P. P.; McManigal, B.; Achalapong, S.; Agarwal, R.; Akech, S.; Albertson, S.; Amuasi, J.; Andrews, J.; Aravkin, A.; Ashley, E.; Babin, F. X.; Bailey, F.; Baker, S.; Basnyat, B.; Bekker, A.; Bender, R.; Berkley, J. A.; Bethou, A.; Bielicki, J.; Boonkasidecha, S.; Bukosia, J.; Carvalheiro, C.; Castañeda-Orjuela, C.; Chansamouth, V.; Chaurasia, S.; Chiurchiù, S.; Chowdhury, F.; Clotaire Donatien, R.; Cook, A. J.; Cooper, B.; Cressey, T. R.; Criollo-Mora, E.; Cunningham, M.; Darboe, S.; Day, N. P. J.; De Luca, M.; Dokova, K.; Dramowski, A.; Dunachie, S. J.; Duong Bich, T.; Eckmanns, T.; Eibach, D.; Emami, A.; Feasey, N.; Fisher-Pearson, N.; Forrest, K.; Garcia, C.; Garrett, D.; Gastmeier, P.; Giref, A. Z.; Greer, R. C.; Gupta, V.; Haller, S.; Haselbeck, A.; Hay, S. I.; Holm, M.; Hopkins, S.; Hsia, Y.; Iregbu, K. C.; Jacobs, J.; Jarovsky, D.; Javanmardi, F.; Jenney, A. W. J.; Khorana, M.; Khusuwan, S.; Kissoon, N.; Kobeissi, E.; Kostyanev, T.; Krapp, F.; Krumkamp, R.; Kumar, A.; Kyu, H. H.; Lim, C.; Lim, K.; Limmathurotsakul, D.; Loftus, M. J.; Lunn, M.; Ma, J.; Manoharan, A.; Marks, F.; May, J.; Mayxay, M.; Mturi, N.; Munera-Huertas, T.; Musicha, P.; Musila, L. A.; Mussi-Pinhata, M. M.; Naidu, R. N.; Nakamura, T.; Nanavati, R.; Nangia, S.; Newton, P.; Ngoun, C.; Novotney, A.; Nwakanma, D.;

Obiero, C. W.; Ochoa, T. J.; Olivas-Martinez, A.; Olliaro, P.; Ooko, E.; Ortiz-Brizuela, E.; Ounchanum, P.; Pak, G. D.; Paredes, J. L.; Peleg, A. Y.; Perrone, C.; Phe, T.; Phommasone, K.; Plakkal, N.; Ponce-de-Leon, A.; Raad, M.; Ramdin, T.; Rattanavong, S.; Riddell, A.; Roberts, T.; Robotham, J. V.; Roca, A.; Rosenthal, V. D.; Rudd, K. E.; Russell, N.; Sader, H. S.; Saengchan, W.; Schnall, J.; et al. Global Burden of Bacterial Antimicrobial Resistance in 2019: A Systematic Analysis. *Lancet* **2022**, *399* (10325), 629−655.

(11) Luepke, K. H.; Suda, K. J.; Boucher, H.; Russo, R. L.; Bonney, M. W.; Hunt, T. D.; Mohr, J. F. Past, Present, and Future of Antibacterial Economics: Increasing Bacterial Resistance, Limited Antibiotic Pipeline, and Societal Implications. *Pharmacotherapy* **2017**, *37* (1), 71−84.

(12) Kwon, J. H.; Powderly, W. G. The Post-Antibiotic Era Is Here. *Science* **2021**, *373* (6554), 471.

(13) Langford, B. J.; So, M.; Raybardhan, S.; Leung, V.; Soucy, J. P. R.; Westwood, D.; Daneman, N.; MacFadden, D. R. Antibiotic Prescribing in Patients with COVID-19: Rapid Review and Meta-Analysis. *Clin. Microbiol. Infect.* **2021**, *27* (4), 520−531.

(14) Mahoney, A. R.; Safaee, M. M.; Wuest, W. M.; Furst, A. L. The Silent Pandemic: Emergent Antibiotic Resistances Following the Global Response to SARS-CoV-2. *iScience* **2021**, *24* (4), 102304.

(15) Lai, C. C.; Shih, T. P.; Ko, W. C.; Tang, H. J.; Hsueh, P. R. Severe Acute Respiratory Syndrome Coronavirus 2 (SARS-CoV-2) and Coronavirus Disease-2019 (COVID-19): The Epidemic and the Challenges. *Int. J. Antimicrob. Agents* **2020**, *55* (3), 105924.

(16) Sreenath, K.; Batra, P.; Vinayaraj, E. V.; Bhatia, R.; SaiKiran, K.; Singh, V.; Singh, S.; Verma, N.; Singh, U. B.; Mohan, A.; Bhatnagar, S.; Trikha, A.; Guleria, R.; Chaudhry, R. Coinfections with Other Respiratory Pathogens among Patients with COVID-19. *Microbiol. Spectrum* **2021**, *9*, 001633.

(17) Mirzaei, R.; Goodarzi, P.; Asadi, M.; Soltani, A.; Aljanabi, H. a. a.; Jeda, A. S.; Dashtbin, S.; Jalalifar, S.; Mohammadzadeh, R.; Teimoori, A.; Tari, K.; Salari, M.; Ghiasvand, S.; Kazemi, S.; Yousefimashouf, R.; Keyvani, H.; Karampoor, S. Bacterial Co-Infections with SARS-CoV-2. *IUBMB Life* **2020**, *72* (10), 2097−2111.

(18) Xu, X. W.; Wu, X. X.; Jiang, X. G.; Xu, K. J.; Ying, L. J.; Ma, C. L.; Li, S. B.; Wang, H. Y.; Zhang, S.; Gao, H. N.; Sheng, J. F.; Cai, H. L.; Qiu, Y. Q.; Li, L. J. Clinical Findings in a Group of Patients Infected with the 2019 Novel Coronavirus (SARS-Cov-2) Outside of Wuhan, China: Retrospective Case Series. *BMJ [Br. Med. J.]* **2020**, *368*, m606.

(19) Granata, G.; Schiavone, F.; Pipitone, G.; Taglietti, F.; Petrosillo, N. Antibiotics Use in COVID-19 Patients: A Systematic Literature Review. *J. Clin. Med.* **2022**, *11* (23), 7207.

(20) Giannella, M.; Rinaldi, M.; Tesini, G.; Gallo, M.; Cipriani, V.; Vatamanu, O.; Campoli, C.; Toschi, A.; Ferraro, C. S.; Horna, C. S.; Bartoletti, M.; Ambretti, S.; Violante, F.; Viale, P.; Curti, S. Predictive Model for Bacterial Co-Infection in Patients Hospitalized for COVID-19: A Multicenter Observational Cohort Study. *Infection* **2022**, *50* (5), 1243−1253.

(21) Mustafa, L.; Tolaj, I.; Baftiu, N.; Fejza, H. Use of Antibiotics in COVID-19 ICU Patients. *J. Infect. Dev. Ctries* **2021**, *15* (04), 501−505.

(22) Gwynn, M. N.; Portnoy, A.; Rittenhouse, S. F.; Payne, D. J. Challenges of Antibacterial Discovery Revisited. *Ann. N.Y. Acad. Sci.* **2010**, *1213* (1), 5−19.

(23) White, A. R.; Blaser, M.; Carrs, O.; Cassell, G.; Fishman, N.; Guidos, R.; Levy, S.; Powers, J.; Norrby, R.; Tillotson, G.; Davies, R.; Projan, S.; Dawson, M.; Monnet, D.; Keogh-brown, M.; Hand, K.; Garner, S.; Findlay, D.; Morel, C.; Wise, R.; Bax, R.; Burke, F.; Chopra, I.; Czaplewski, L.; Finch, R.; Livermore, D.; Piddock, L. J. V.; White, T. Effective Antibacterials: At What Cost? The Economics of Antibacterial Resistance and Its Control. *J. Antimicrob. Chemother.* **2011**, *66* (9), 1948−1953.

(24) Projan, S. J. Why Is Big Pharma Getting out of Antibacterial Drug Discovery? *Curr. Opin. Microbiol.* **2003**, *6* (5), 427−430.

(25) Brown, E. D.; Wright, G. D. Antibacterial Drug Discovery in the Resistance Era. *Nature* **2016**, *529* (7586), 336−343.

(26) Hutchings, M.; Truman, A.; Wilkinson, B. Antibiotics: Past, Present and Future. *Curr. Opin. Microbiol.* **2019**, *51*, 72−80.

(27) WHO. *2020 Antibacterial Agents in Clinical and Preclinical Development*, 2021.

(28) Butler, M. S.; Gigante, V.; Sati, H.; Paulin, S.; Al-Sulaiman, L.; Rex, J. H.; Fernandes, P.; Arias, C. A.; Paul, M.; Thwaites, G. E.; Czaplewski, L.; Alm, R. A.; Lienhardt, C.; Spigelman, M.; Silver, L. L.; Ohmagari, N.; Kozlov, R.; Harbarth, S.; Beyer, P. Analysis of the Clinical Pipeline of Treatments for Drug-Resistant Bacterial Infections: Despite Progress, More Action Is Needed. *Antimicrob. Agents Chemother.* **2022**, *66* (3), 019911.

(29) Beyer, P.; Paulin, S. The Antibacterial Research and Development Pipeline Needs Urgent Solutions. *ACS Infect. Dis.* **2020**, *6* (6), 1289−1291.

(30) Butler, M. S.; Henderson, I. R.; Capon, R. J.; Blaskovich, M. A. T. Antibiotics in the Clinical Pipeline as of December 2022. *J. Antibiot.* **2023**, *76*, 431−473.

(31) Clement, J. L.; Jarrett, P. S. Antibacterial Silver. *Met.-Based Drugs* **1994**, *1* (5−6), 467−482.

(32) Russell, A. D.; Hugo, W. B. 7 Antimicrobial Activity and Action of Silver. *Prog. Med. Chem.* **1994**, *31* (C), 351−370.

(33) Strebhardt, K.; Ullrich, A. Paul Ehrlich's Magic Bullet Concept: 100 Years of Progress. *Nat. Rev. Cancer* **2008**, *8* (6), 473−480.

(34) Aminov, R. I. A Brief History of the Antibiotic Era: Lessons Learned and Challenges for the Future. *Front. Microbiol.* **2010**, *1*, 134.

(35) Rosenberg, B.; VanCamp, L.; Trosko, J. E.; Mansour, V. H. Platinum Compounds: A New Class of Potent Antitumour Agents. *Nature* **1969**, *222* (5191), 385−386.

(36) Siddik, Z. H. Cisplatin: Mode of Cytotoxic Action and Molecular Basis of Resistance. *Oncogene* **2003**, *22*, 7265−7279.

(37) Florea, A. M.; Büsselberg, D. Cisplatin as an Anti-Tumor Drug: Cellular Mechanisms of Activity, Drug Resistance and Induced Side Effects. *Cancers* **2011**, *3* (1), 1351−1371.

(38) Rosenberg, B.; Van Camp, L.; Krigas, T. Inhibition of Cell Division in Escherichia Coli by Electrolysis Products from a Platinum Electrode. *Nature* **1965**, *205* (4972), 698−699.

(39) Dwyer, F. P.; Gyarfas, E. C.; Rogers, W. P.; Koch, J. H. Biological Activity of Complex Ions. *Nature* **1952**, *170* (4318), 190−191.

(40) Dwyer, F. P.; Reid, I. K.; Shulman, A.; Laycock, G. M.; Dixson, S. The Biological Actions of 1,10-Phenanthroline and 2,2'-Bipyridine Hydrochlorides, Quaternary Salts and Metal Chelates and Related Compounds. 1. Bacteriostatic Action on Selected Gram-Positive, Gram-Negative and Acid-Fast Bacteria. *Aust. J. Exp. Biol. Med. Sci.* **1969**, *47* (2), 203−218.

(41) Butler, H. M.; Laver, J. C.; Shulman, A.; Wright, R. D. The Use of Phenanthroline Metal Chelates for the Control of Topical Infections Due to Bacteria, Fungi and Protozoa. *Med. J. Aust.* **1970**, *2* (7), 309−314.

(42) Li, F.; Mulyana, Y.; Feterl, M.; Warner, J. M.; Collins, J. G.; Keene, F. R. The Antimicrobial Activity of Inert Oligonuclear Polypyridylruthenium(II) Complexes against Pathogenic Bacteria, Including MRSA. *Dalton Trans.* **2011**, *40* (18), 5032−5038.

(43) Li, F.; Collins, J. G.; Keene, F. R. Ruthenium Complexes as Antimicrobial Agents. *Chem. Soc. Rev.* **2015**, *44* (8), 2529−2542.

(44) Li, X.; Gorle, A. K.; Sundaraneedi, M. K.; Keene, F. R.; Collins, J. G. Kinetically-Inert Polypyridylruthenium(II) Complexes as Therapeutic Agents. *Coord. Chem. Rev.* **2018**, *375*, 134−147.

(45) Frei, A.; Zuegg, J.; Elliott, A. G.; Baker, M.; Braese, S.; Brown, C.; Chen, F. G.; G Dowson, C.; Dujardin, G.; Jung, N.; King, A. P.; Mansour, A. M.; Massi, M.; Moat, J.; Mohamed, H. A.; Renfrew, A. K.; Rutledge, P. J.; Sadler, P. J.; Todd, M. H.; Willans, C. E.; Wilson, J. J.; Cooper, M. A.; Blaskovich, M. A. T. Metal Complexes as a Promising Source for New Antibiotics. *Chem. Sci.* **2020**, *11* (10), 2627−2639.

(46) Frei, A. Metal Complexes, an Untapped Source of Antibiotic Potential? *Antibiotics* **2020**, *9* (2), 90.

(47) Nasiri Sovari, S.; Zobi, F. Recent Studies on the Antimicrobial Activity of Transition Metal Complexes of Groups 6–12. *Chemistry* **2020**, 2 (2), 418–452.

(48) Biegański, P.; Szczupak, Ł.; Arruebo, M.; Kowalski, K. Brief Survey on Organometalated Antibacterial Drugs and Metal-Based Materials with Antibacterial Activity. *RSC Chem. Biol.* **2021**, 2 (2), 368–386.

(49) Liang, J.; Sun, D.; Yang, Y.; Li, M.; Li, H.; Chen, L. Discovery of Metal-Based Complexes as Promising Antimicrobial Agents. *Eur. J. Med. Chem.* **2021**, 224, 113696.

(50) Yousuf, I.; Bashir, M.; Arjmand, F.; Tabassum, S. Advancement of Metal Compounds as Therapeutic and Diagnostic Metallodrugs: Current Frontiers and Future Perspectives. *Coord. Chem. Rev.* **2021**, 445, 214104.

(51) Ali, F.; Aute, S.; Sreedharan, S.; Anila, H. A.; Saeed, H. K. *Specific HOCl Tracking across Diverse Cellular Organelles in Real Time Using a Superresolution Microscopy Probe*, 2018.

(52) Singh, H.; Sreedharan, S.; Oyarzabal, E.; Mahapatra, T. S.; Green, N.; Shih, Y. Y. I.; Das, M.; Thomas, J. A.; Pramanik, S. K.; Das, A. Mitochondriotropic Lanthanide Nanorods: Implications for Multimodal Imaging. *Chem. Commun.* **2020**, 56 (57), 7945–7948.

(53) Sreedharan, S.; Gill, M. R.; Garcia, E.; Saeed, H. K.; Robinson, D.; Byrne, A.; Cadby, A.; Keyes, T. E.; Smythe, C.; Pellett, P.; Bernardino De La Serna, J.; Thomas, J. A. Multimodal Super-Resolution Optical Microscopy Using a Transition-Metal-Based Probe Provides Unprecedented Capabilities for Imaging Both Nuclear Chromatin and Mitochondria. *J. Am. Chem. Soc.* **2017**, 139 (44), 15907–15913.

(54) Dröge, F.; Noakes, F. F.; Archer, S. A.; Sreedharan, S.; Raza, A.; Robertson, C. C.; MacNeil, S.; Haycock, J. W.; Carson, H.; Meijer, A. J. H. M.; Smythe, C. G. W.; Bernardino De La Serna, J.; Dietzek-Ivanšić, B.; Thomas, J. A. A Dinuclear Osmium(II) Complex Near-Infrared Nanoscopy Probe for Nuclear DNA. *J. Am. Chem. Soc.* **2021**, 143 (48), 20442–20453.

(55) Ramu, V.; Gill, M. R.; Jarman, P. J.; Turton, D.; Thomas, J. A.; Das, A.; Smythe, C. A Cytostatic Ruthenium (II)–Platinum (II) Bis (Terpyridyl) Anticancer Complex That Blocks Entry into S Phase by Up-regulating P27KIP1. *Chem.—Eur. J.* **2015**, 21 (25), 9185–9197.

(56) Gill, M. R.; Jarman, P. J.; Halder, S.; Walker, M. G.; Saeed, H. K.; Thomas, J. A.; Smythe, C.; Ramadan, K.; Vallis, K. A. A Three-in-One-Bullet for Oesophageal Cancer: Replication Fork Collapse, Spindle Attachment Failure and Enhanced Radiosensitivity Generated by a Ruthenium(II) Metallo-Intercalator. *Chem. Sci.* **2018**, 9 (4), 841–849.

(57) Jarman, P. J.; Noakes, F.; Fairbanks, S.; Smitten, K.; Griffiths, I. K.; Saeed, H. K.; Thomas, J. A.; Smythe, C. Exploring the Cytotoxicity, Uptake, Cellular Response, and Proteomics of Mono- and Dinuclear DNA Light-Switch Complexes. *J. Am. Chem. Soc.* **2019**, 141 (7), 2925–2937.

(58) Archer, S. A.; Raza, A.; Dröge, F.; Robertson, C.; Auty, A. J.; Chekulaev, D.; Weinstein, J. A.; Keane, T.; Meijer, A. J. H. M.; Haycock, J. W.; Macneil, S.; Thomas, J. A. A Dinuclear Ruthenium-(II) Phototherapeutic That Targets Duplex and Quadruplex DNA. *Chem. Sci.* **2019**, 10 (12), 3502–3513.

(59) Raza, A.; Archer, S. A.; Fairbanks, S. D.; Smitten, K. L.; Botchway, S. W.; Thomas, J. A.; MacNeil, S.; Haycock, J. W. A Dinuclear Ruthenium(II) Complex Excited by Near-Infrared Light through Two-Photon Absorption Induces Phototoxicity Deep within Hypoxic Regions of Melanoma Cancer Spheroids. *J. Am. Chem. Soc.* **2020**, 142 (10), 4639–4647.

(60) Saeed, H. K.; Jarman, P. J.; Archer, S.; Sreedharan, S.; Saeed, I. Q.; Mckenzie, L. K.; Weinstein, J. A.; Buurma, N. J.; Smythe, C. G. W.; Thomas, J. A. Homo- and Heteroleptic Phototoxic Dinuclear Metallo-Intercalators Based on RuII(Dppn) Intercalating Moieties: Synthesis, Optical, and Biological Studies. *Angew. Chem., Int. Ed.* **2017**, 56 (41), 12628–12633.

(61) Saeed, H. K.; Sreedharan, S.; Jarman, P. J.; Archer, S. A.; Fairbanks, S. D.; Foxon, S. P.; Auty, A. J.; Chekulaev, D.; Keane, T.; Meijer, A. J. H. M. H. M.; Weinstein, J. A.; Smythe, C. G. W.; Bernardino De La Serna, J.; Thomas, J. A. Making the Right Link to Theranostics: The Photophysical and Biological Properties of Dinuclear Ru^{II}-Re^{I} Dppz Complexes Depend on Their Tether. *J. Am. Chem. Soc.* **2020**, 142 (2), 1101–1111.

(62) Smitten, K. L.; Southam, H. M.; de la Serna, J. B.; Gill, M. R.; Jarman, P. J.; Smythe, C. G. W. W.; Poole, R. K.; Thomas, J. A. Using Nanoscopy to Probe the Biological Activity of Antimicrobial Leads That Display Potent Activity against Pathogenic, Multidrug Resistant, Gram-Negative Bacteria. *ACS Nano* **2019**, 13 (5), 5133–5146.

(63) Varney, A. M.; Smitten, K. L.; Thomas, J. A.; Mclean, S. Transcriptomic Analysis of the Activity and Mechanism of Action of a Ruthenium(II)-Based Antimicrobial That Induces Minimal Evolution of Pathogen Resistance. *ACS Pharmacol. Transl. Sci.* **2021**, 4 (1), 168–178.

(64) Smitten, K. L.; Fairbanks, S. D.; Robertson, C. C.; Bernardino De La Serna, J.; Foster, S. J.; Thomas, J. A. Ruthenium Based Antimicrobial Theranostics-Using Nanoscopy to Identify Therapeutic Targets and Resistance Mechanisms in: Staphylococcus Aureus. *Chem. Sci.* **2020**, 11 (1), 70–79.

(65) Smitten, K. L.; Thick, E. J.; Southam, H. M.; Bernardino de la Serna, J.; Foster, S. J.; Thomas, J. A. Mononuclear Ruthenium(II) Theranostic Complexes That Function as Broad-Spectrum Antimicrobials in Therapeutically Resistant Pathogens through Interaction with DNA. *Chem. Sci.* **2020**, 11 (33), 8828–8838.

(66) Drlica, K.; Malik, M. Fluoroquinolones: Action and Resistance. *Curr. Top. Med. Chem.* **2003**, 3 (3), 249–282.

(67) Miert, A. S. J. P. A. M. V. The Sulfonamide-diaminopyrimidine Story. *J. Vet. Pharmacol. Ther.* **1994**, 17 (4), 309–316.

(68) Bolhuis, A.; Hand, L.; Marshall, J. E.; Richards, A. D.; Rodger, A.; Aldrich-Wright, J. Antimicrobial Activity of Ruthenium-Based Intercalators. *Eur. J. Pharm. Sci.* **2011**, 42 (4), 313–317.

(69) Bolhuis, A.; Aldrich-Wright, J. R. DNA as a Target for Antimicrobials. *Bioorg. Chem.* **2014**, 55 (C), 51–59.

(70) Varney, A. M.; Mannix-fisher, E.; Thomas, J. C.; McLean, S. Evaluation of Phenotypic and Genotypic Methods for the Identification and Characterisation of Bacterial Isolates Recovered from Catheter-Associated Urinary Tract Infections. *J. Appl. Microbiol.* **2023**, 12 (11), 571106.

(71) Brooks, T.; Keevil, C. W. C. A simple artificial urine for the growth of urinary pathogens. *Lett. Appl. Microbiol.* **1997**, 24 (3), 203–206.

(72) Ackermann, T.; Tardito, S. Cell Culture Medium Formulation and Its Implications in Cancer Metabolism. *Trends Cancer* **2019**, 5, 329–332.

(73) Vande Voorde, J.; Ackermann, T.; Pfetzer, N.; Sumpton, D.; Mackay, G.; Kalna, G.; Nixon, C.; Blyth, K.; Gottlieb, E.; Tardito, S. Improving the Metabolic Fidelity of Cancer Models with a Physiological Cell Culture Medium. *Sci. Adv.* **2019**, 5 (1), No. eaau7314.

(74) Lam, P. L.; Lu, G. L.; Hon, K. M.; Lee, K. W.; Ho, C. L.; Wang, X.; Tang, J. C. O.; Lam, K. H.; Wong, R. S. M.; Kok, S. H. L.; Bian, Z. X.; Li, H.; Lee, K. K. H.; Gambari, R.; Chui, C. H.; Wong, W. Y. Development of Ruthenium(II) Complexes as Topical Antibiotics against Methicillin Resistant Staphylococcus Aureus. *Dalton Trans.* **2014**, 43 (10), 3949–3957.

(75) Gorle, A. K.; Feterl, M.; Warner, J. M.; Wallace, L.; Keene, F. R.; Collins, J. G. Tri- and Tetra-Nuclear Polypyridyl Ruthenium(Ii) Complexes as Antimicrobial Agents. *Dalton Trans.* **2014**, 43 (44), 16713–16725.

(76) Kumar, S. V.; Scottwell, S. O.; Waugh, E.; McAdam, C. J.; Hanton, L. R.; Brooks, H. J. L.; Crowley, J. D. Antimicrobial Properties of Tris(Homoleptic) Ruthenium(II) 2-Pyridyl-1,2,3-Triazole "Click" Complexes against Pathogenic Bacteria, Including Methicillin-Resistant Staphylococcus Aureus (MRSA). *Inorg. Chem.* **2016**, 55 (19), 9767–9777.

(77) Li, F.; Feterl, M.; Mulyana, Y.; Warner, J. M.; Collins, J. G.; Keene, F. R. In Vitro Susceptibility and Cellular Uptake for a New Class of Antimicrobial Agents: Dinuclear Ruthenium(II) Complexes. *J. Antimicrob. Chemother.* **2012**, 67 (11), 2686–2695.

(78) Matshwele, J. T. P.; Nareetsile, F.; Mapolelo, D.; Matshameko, P.; Leteane, M.; Nkwe, D. O.; Odisitse, S. Synthesis of Mixed Ligand Ruthenium (II/III) Complexes and Their Antibacterial Evaluation on Drug-Resistant Bacterial Organisms. *J. Chem.* **2020**, *2020*, 1−10.

(79) Fey, P. D.; Endres, J. L.; Yajjala, V. K.; Widhelm, T. J.; Boissy, R. J.; Bose, J. L.; Bayles, K. W. A Genetic Resource for Rapid and Comprehensive Phenotype Screening of Nonessential Staphylococcus Aureus Genes. *MBio* **2013**, *4* (1), 005377.

(80) Ramarao, N.; Nielsen-Leroux, C.; Lereclus, D. The Insect Galleria Mellonella as a Powerful Infection Model to Investigate Bacterial Pathogenesis. *J. Visualized Exp.* **2012**, No. 70, No. e4392.

(81) Tsai, C. J. Y.; Loh, J. M. S.; Proft, T. Galleria Mellonella Infection Models for the Study of Bacterial Diseases and for Antimicrobial Drug Testing. *Virulence* **2016**, *7* (3), 214−229.

(82) Piatek, M.; Sheehan, G.; Kavanagh, K. Utilising Galleria Mellonella Larvae for Studying in Vivo Activity of Conventional and Novel Antimicrobial Agents. *Pathog. Dis.* **2020**, *78* (8), ftaa059.

(83) Piatek, M.; Sheehan, G.; Kavanagh, K. Galleria Mellonella: The Versatile Host for Drug Discovery, in Vivo Toxicity Testing and Characterising Host-Pathogen Interactions. *Antibiotics* **2021**, *10* (12), 1545.

(84) Bolouri Moghaddam, M. R.; Tonk, M.; Schreiber, C.; Salzig, D.; Czermak, P.; Vilcinskas, A.; Rahnamaeian, M. The Potential of the Galleria Mellonella Innate Immune System Is Maximized by the Co-Presentation of Diverse Antimicrobial Peptides. *Biol. Chem.* **2016**, *397* (9), 939−945.

(85) Wojda, I. Immunity of the Greater Wax Moth Galleria Mellonella. *Insect Sci.* **2017**, *24* (3), 342−357.

(86) Dinh, H.; Semenec, L.; Kumar, S. S.; Short, F. L.; Cain, A. K. Microbiology's next Top Model: Galleria in the Molecular Age. *Pathog. Dis.* **2021**, *79* (2), ftab006.

(87) Smitten, K.; Southam, H. M.; Fairbanks, S.; Graf, A.; Chauvet, A.; Thomas, J. A. Clearing an ESKAPE Pathogen in a Model Organism; A Polypyridyl Ruthenium(II) Complex Theranostic That Treats a Resistant Acinetobacter Baumannii Infection in Galleria Mellonella. *Chem.—Eur. J.* **2023**, *29* (11), No. e202203555.

(88) Dijkshoorn, L.; Nemec, A.; Seifert, H. An Increasing Threat in Hospitals: Multidrug-Resistant Acinetobacter Baumannii. *Nat. Rev. Microbiol.* **2007**, *5* (12), 939−951.

(89) Sarshar, M.; Behzadi, P.; Scribano, D.; Palamara, A. T.; Ambrosi, C. Acinetobacter Baumannii: An Ancient Commensal with Weapons of a Pathogen. *Pathogens* **2021**, *10* (4), 387.

(90) Isler, B.; Doi, Y.; Bonomo, R. A.; Paterson, D. L. New Treatment Options against Carbapenem-Resistant Acinetobacter Baumannii Infections. *Antimicrob. Agents Chemother.* **2019**, *63* (1), e01110−e01118.

(91) Alrahmany, D.; Omar, A. F.; Alreesi, A.; Harb, G.; Ghazi, I. M. Acinetobacter Baumannii Infection-Related Mortality in Hospitalized Patients: Risk Factors and Potential Targets for Clinical and Antimicrobial Stewardship Interventions. *Antibiotics* **2022**, *11* (8), 1086.

(92) Cavallo, I.; Oliva, A.; Pages, R.; Sivori, F.; Truglio, M.; Fabrizio, G.; Pasqua, M.; Pimpinelli, F.; Di Domenico, E. G. Acinetobacter Baumannii in the Critically Ill: Complex Infections Get Complicated. *Front. Microbiol.* **2023**, *14*, 1196774.

(93) Gordon, N. C.; Png, K.; Wareham, D. W. Potent Synergy and Sustained Bactericidal Activity of a Vancomycin-Colistin Combination versus Multidrug-Resistant Strains of Acinetobacter Baumannii. *Antimicrob. Agents Chemother.* **2010**, *54* (12), 5316−5322.

(94) Rubinstein, E. Short Antibiotic Treatment Courses or How Short Is Short? *Int. J. Antimicrob. Agents* **2007**, *30*, S76−S79.

(95) Spellberg, B.; Rice, L. B. Duration of Antibiotic Therapy: Shorter Is Better. *Ann. Intern. Med.* **2019**, *171* (3), 210−211.

(96) Alcock, B. P.; Huynh, W.; Chalil, R.; Smith, K. W.; Raphenya, A. R.; Wlodarski, M. A.; Edalatmand, A.; Petkau, A.; Syed, S. A.; Tsang, K. K.; Baker, S. J. C.; Dave, M.; Mccarthy, M. C.; Mukiri, K. M.; Nasir, J. A.; Golbon, B.; Imtiaz, H.; Jiang, X.; Kaur, K.; Kwong, M.; Liang, Z. C.; Niu, K. C.; Shan, P.; Yang, J. Y. J.; Gray, K. L.; Hoad, G. R.; Jia, B.; Bhando, T.; Carfrae, L. A.; Farha, M. A.; French, S.; Gordzevich, R.; Rachwalski, K.; Tu, M. M.; Bordeleau, E.; Dooley, D.; Griffiths, E.; Zubyk, H. L.; Brown, E. D.; Maguire, F.; Beiko, R. G.; Hsiao, W. W. L.; Brinkman, F. S. L.; Van Domselaar, G.; Mcarthur, A. G. CARD 2023: Expanded Curation, Support for Machine Learning, and Resistome Prediction at the Comprehensive Antibiotic Resistance Database. *Nucleic Acids Res.* **2023**, *51*, D690−D699.

(97) Liu, B.; Zheng, D.; Jin, Q.; Chen, L.; Yang, J. VFDB 2019: A Comparative Pathogenomic Platform with an Interactive Web Interface. *Nucleic Acids Res.* **2019**, *47* (D1), D687−D692.

(98) Wishart, D. S.; Han, S.; Saha, S.; Oler, E.; Peters, H.; Grant, J. R.; Stothard, P.; Gautam, V. PHASTEST: Faster than PHASTER, Better than PHAST. *Nucleic Acids Res.* **2023**, *51* (W1), W443−W450.

(99) Antimicrobial Susceptibility Testing. In *Clinical Microbiology Procedures Handbook*; Leber, A. L., ed.; 2010; pp 5.0.1−5.18.2.1.

(100) Harding, C. R.; Schroeder, G. N.; Collins, J. W.; Frankel, G. Use of Galleria Mellonella as a Model Organism to Study Legionella Pneumophila Infection. *J. Visualized Exp.* **2013**, *81* (81), No. e50964.